

RESEARCH ARTICLE

# Drosophila ZDHHC8 palmitoylates scribble and Ras64B and controls growth and viability

Katrin Strassburger<sup>1,2</sup>, Evangeline Kang<sup>1,2</sup>, Aurelio A. Teleman<sup>1,2\*</sup>

**1** German Cancer Research Center (DKFZ), Heidelberg, Germany, **2** Heidelberg University, Heidelberg, Germany

\* [a.teleman@dkfz.de](mailto:a.teleman@dkfz.de)



## Abstract

Palmitoylation is an important posttranslational modification regulating diverse cellular functions. Consequently, aberrant palmitoylation can lead to diseases such as neuronal disorders or cancer. In humans there are roughly one hundred times more palmitoylated proteins than enzymes catalyzing palmitoylation (palmitoyltransferases). Therefore, it is an important challenge to establish the links between palmitoyltransferases and their targets. From publicly available data, we find that expression of human ZDHHC8 correlates significantly with cancer survival. To elucidate the organismal function of ZDHHC8, we study the Drosophila ortholog of hZDHHC8, CG34449/dZDHHC8. Knockdown of dZDHHC8 causes tissue overgrowth while dZDHHC8 mutants are larval lethal. We provide a list of 159 palmitoylated proteins in Drosophila and present data suggesting that scribble and Ras64B are targets of dZDHHC8.

## OPEN ACCESS

**Citation:** Strassburger K, Kang E, Teleman AA (2019) Drosophila ZDHHC8 palmitoylates scribble and Ras64B and controls growth and viability. PLoS ONE 14(2): e0198149. <https://doi.org/10.1371/journal.pone.0198149>

**Editor:** F. Gisou van der Goot, Ecole Polytechnique Federale de Lausanne, SWITZERLAND

**Received:** May 8, 2018

**Accepted:** January 24, 2019

**Published:** February 8, 2019

**Copyright:** © 2019 Strassburger et al. This is an open access article distributed under the terms of the [Creative Commons Attribution License](https://creativecommons.org/licenses/by/4.0/), which permits unrestricted use, distribution, and reproduction in any medium, provided the original author and source are credited.

**Data Availability Statement:** All relevant data are within the paper and its Supporting Information files.

**Funding:** This work was partially funded by Helmholtz Postdoc Programm. The funder had no role in study design, data collection and analysis, decision to publish, or preparation of the manuscript.

**Competing interests:** The authors have declared that no competing interests exist.

## Introduction

Next generation sequencing technology has allowed the broad sequencing of tumors and adjacent healthy tissues to identify cancer-linked somatic mutations and cancer-linked genes. Many of these genes, however, are functionally uncharacterized and a role in cancer development has not been tested. This would be necessary to distinguish cancer ‘driver mutations’ from ‘passenger mutations’ which occur by chance and are neutral for the cancer phenotype. Drosophila is a good model organism for understanding gene function as the generation of loss-of-function mutants is fast, cancer-like phenotypes can be easily assayed, and flies have less genetic redundancy compared to humans, allowing the easier identification of phenotypes.

We focus here on a protein belonging to the family of palmitoyltransferases, which can be recognized in part due to their zinc finger DHHC domain (ZDHHC). ZDHHC enzymes catalyze the posttranslational, covalent attachment of the long chain acyl chains palmitate (C16:0) and stearate (C18:0) to cysteines of target proteins (S-palmitoylation). The binding of C16:0 to cysteines occurs via thioester linkages and can be reverted by thioesterases. Since S-palmitoylation is reversible and dynamic it can control a number of cellular processes such as subcellular trafficking, protein localization and stability as well as enzyme activity [1–3]. In mammals 23

proteins of the DHHC family have been identified as well as roughly 2000 palmitoylated proteins [4]. Therefore, it is an important challenge to understand which palmitoyltransferase targets which substrate.

Aberrant palmitoylation has been linked to many diseases ranging from neuronal disorders [5,6] to cancer [4,7–10]. Well known oncogenes whose activity is controlled by palmitoylation are for instance H-Ras and N-Ras proteins [11]. Recently, epidermal growth factor receptor (EGFR) has been shown to be palmitoylated by DHHC20 and loss of palmitoylation leads to increased EGFR signaling, cell migration and transformation [12]. DHHC3 was shown to have growth promoting effects in breast cancer cells regulating oxidative stress and senescence [13]. Consequently, palmitoyltransferases are being pursued as targets for therapeutic intervention in cancer [14].

We show here that knockdown of the *Drosophila* orthologue of human ZDHHC8 (CG34449 or dZDHHC8) causes tissue overgrowth. dZDHHC8 mutants are larval lethal and have metabolic phenotypes. We identify potential targets of dZDHHC8 and suggest that dZDHHC8 loss of function phenotypes partly arise from decreased palmitoylation of scribble and Ras64B proteins.

## Results

### *Drosophila* ZDHHC8 knockdown causes tissue overgrowth

We aimed to functionally characterize novel cancer relevant genes. To identify such genes we searched through publicly available databases for genes whose expression correlates with patient survival. In The Protein Atlas database ([www.proteinatlas.org](http://www.proteinatlas.org)) [15] we found that the expression of ZDHHC8 correlates with cancer prognosis (S1A Fig). In renal and cervical cancer, high expression of ZDHHC8 is significantly correlated with shorter survival times, whereas in lung and pancreatic cancers high expression significantly correlates with longer survival rates (S1A Fig). These data suggest that ZDHHC8 may play a role in cancer incidence and/or progression, but that this role likely depends on tumor type or context. Since ZDHHC8 has not been previously linked to these cancers we decided to study ZDHHC8 function, and whether it affects tissue growth or cell proliferation.

ZDHHC8 is a member of the palmitoyl-transferase group that is highly conserved across evolution. BLASTing the protein sequence of human ZDHHC8 against the *Drosophila* proteome identifies the uncharacterized gene CG34449 as a top hit with an E-value of  $10^{-76}$  (S1B Fig). Conversely, a BLAST search of the human proteome using CG34449 protein sequences identifies ZDHHC8 as the top hit with an E-value of  $10^{-87}$  (S1B Fig). Hence, CG34449 is the *Drosophila* orthologue of hZDHHC8. We therefore used *Drosophila melanogaster* as a model system to study CG34449 function *in vivo* and refer to it as dZDHHC8.

We first tested whether dZDHHC8 regulates tissue growth in the *Drosophila* wing, since the wing is flat and its size is easily quantified. The wing consists of two cellular layers, a dorsal and a ventral layer (Fig 1A). Unbalanced growth of the two layers leads to bending of the wing. We knocked down dZDHHC8 with three independent RNAi lines, targeting different regions of the gene in the dorsal part of the wing using the apterous-Gal4 driver (apG4) (Fig 1A). In all three cases we observed a downward bending of the wings, indicating that knockdown of dZDHHC8 leads to tissue overgrowth (Fig 1A). Since we observe this phenotype with three independent dsRNA's, this makes it highly unlikely that off-target effects are responsible for the phenotype. Immunostaining of wing discs with anti-dZDHHC8 antibody confirmed that the RNAi constructs efficiently reduced ZDHHC8 protein levels in the dorsal compartment, hence the mild phenotype is unlikely to be due to inefficient knockdown (S2A Fig). Also when dZDHHC8 is knocked down in the posterior part of the wing using the engrailed-Gal4 driver,

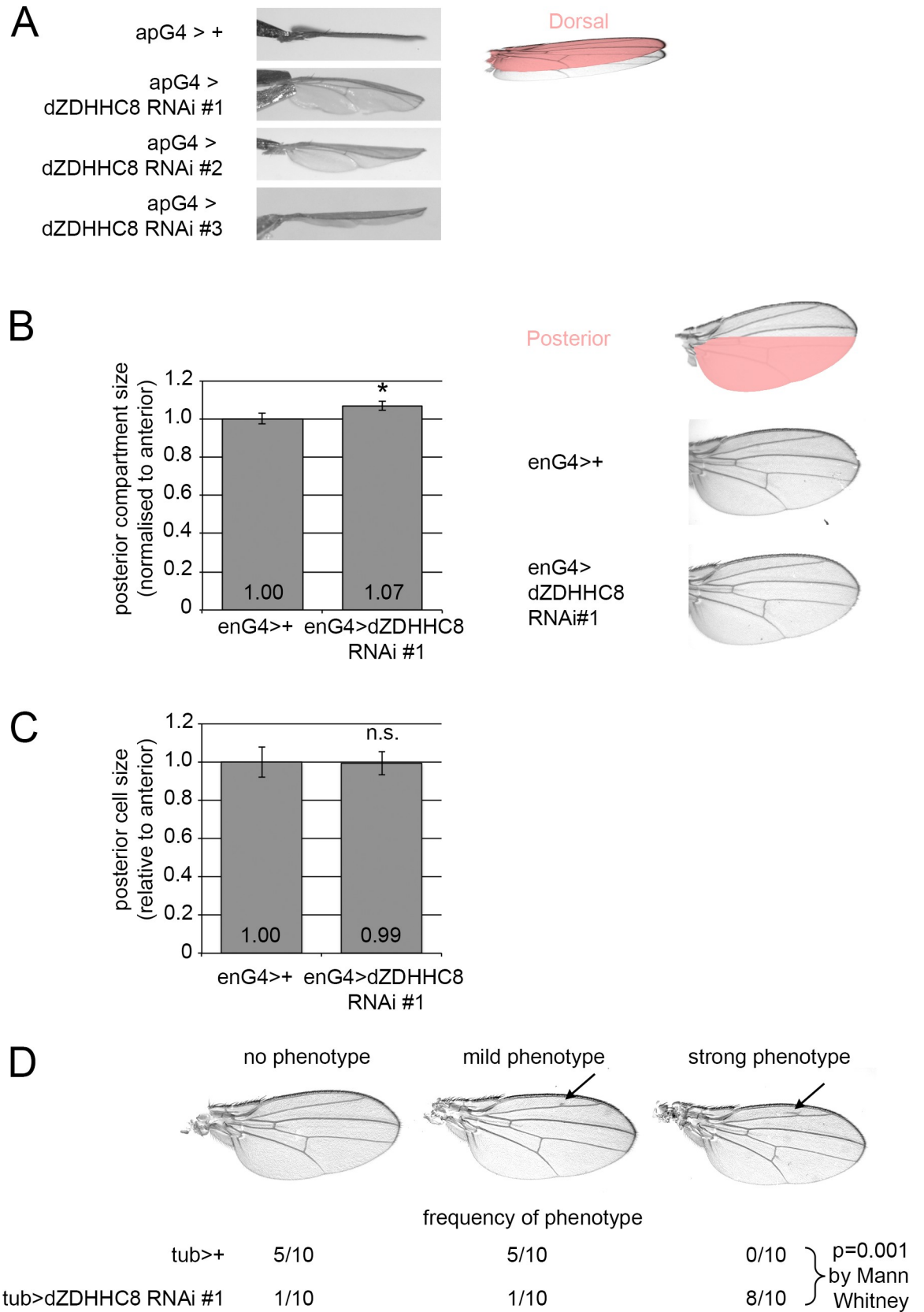


**Fig 1. dZDHHHC8 knockdown causes tissue overgrowth due to increased cell proliferation.** (A) Three independent RNAi lines targeting different regions of dZDHHHC8 mRNA result in tissue overgrowth and downward bending of the wing when expressed in the dorsal compartment using apterous-Gal4 (apG4) at 25°C. Phenotype penetrance = 100% (26/26 for RNAi #1, 23/23 for RNAi #2, 32/32 for RNAi #3). (B) Expression of dZDHHHC8 RNAi in the posterior compartment of the wing using engrailed-Gal4 (enG4>dZDHHHC8 RNAi #1) increases posterior compartment size normalized to anterior when compared to control wings (enG4>+). Representative examples are provided on the right. Phenotype penetrance = 90% (1 of 10 RNAi wings had a P/A ratio smaller than the largest P/A ratio of control wings.) Error bars = stdev. n≥9. \* ttest = 2x10<sup>-5</sup>. (C) The size of wing cells is not altered upon dZDHHHC8 knockdown suggesting that tissue overgrowth is caused by enhanced cell proliferation. dZDHHHC8 is knocked down in the posterior compartment with engrailed-Gal4 (enG4>dZDHHHC8 RNAi #1). Cell size was determined by counting the number of cells (via trichomes) within a wing area of defined size. Error bars = stdev. n≥9. (D) Ubiquitous expression of dZDHHHC8 RNAi using tubulin-Gal4 (tubG4>GFP, dZDHHHC8 RNAi #2) often results in formation of extra vein material. Frequency of phenotypes in adult males of indicated genotypes are shown below representative images.

<https://doi.org/10.1371/journal.pone.0198149.g001>

(enG4>dZDHHHC8 RNAi #1, Fig 1B) the ratio of posterior to anterior wing size increases mildly (7%) but significantly compared to control wings (enG4>+, Fig 1B). The overgrowth phenotype did not become stronger at 29°C (where the GAL4/UAS system is more active) (S2B Fig) or by using the stronger hedgehog-Gal4 driver (S2C Fig), suggesting the knockdown is efficient in these conditions. To find out whether this increased tissue size is due to more cells or larger cells, we quantified cell size in the posterior compartment where dZDHHHC8 was knocked down and normalized it to cell size in the control anterior compartment. This was done by counting the number of cells via trichomes in a region of defined size, and then calculating the ratio of area per cell. We found that cell size was not affected by dZDHHHC8 knockdown (enG4>dZDHHHC8 RNAi, Fig 1C) when compared to control wings (enG4>+, Fig 1C). Representative examples are shown in S2D Fig. This suggests that the increased tissue size is due enhanced cell proliferation upon dZDHHHC8 knockdown. Knocking down dZDHHHC8 ubiquitously using tubulin-Gal4 (tubG4>GFP, dZDHHHC8 RNAi, Fig 1D) resulted in extra vein material, which was significantly less prominent in control wings (tubG4>+, Fig 1D).

### dZDHHHC8 knockouts are larval lethal with metabolic phenotypes

To further study the function of dZDHHHC8 we generated two different knockout alleles. Knockout line 1 (KO1) lacks most of the dZDHHHC8 genomic sequence, including CG34450, which is annotated as a separate gene within dZDHHHC8 in Flybase (Fig 2A) [16]. Since these two genes were previously annotated in Flybase as one linked gene and split into two genes in release 5.2 of the genome annotation, we tested whether they are indeed independent of each other. We knocked down CG34450 in Drosophila S2 cells and measured levels of dZDHHHC8 mRNA by qRT-PCR using oligos that anneal to different regions of dZDHHHC8 (S3 Fig). Knockdown of CG34450 caused mRNA levels of both CG34450 and dZDHHHC8 to drop (S3 Fig). Transcript levels of dZDHHHC8 decreased less than levels of CG34450 transcript, although this could be explained by the fact that dZDHHHC8 has multiple alternatively-spliced transcript isoforms (Fig 2A). This indicates that mRNA levels of dZDHHHC8 and CG34450 are linked in some way and perhaps they are not separate genes. In a second knockout line we removed a small genomic region common to all isoforms of dZDHHHC8 including the catalytic domain (KO2 Fig 2A). We confirmed that dZDHHHC8 knockouts do not have dZDHHHC8 protein by western blot analysis using a dZDHHHC8 antibody which we raised in guinea pigs (Fig 2B). (The expected molecular weights of dZDHHHC8 are 54kD, 57kD, 91kD, 97kD, 100kD and 113kD, depending on the splice isoform. Furthermore, integral membrane proteins such as ZDHHHC8 often forms multiple bands on an SDS-PAGE gel.)

Both dZDHHHC8<sup>KO1</sup> and dZDHHHC8<sup>KO2</sup> animals do not reach adulthood, but die as larvae. To determine precisely at which stage dZDHHHC8<sup>KO1</sup> animals die, we collected control (CT) or dZDHHHC8<sup>KO1</sup> newly-hatched first-instar larvae and examined the number and developmental

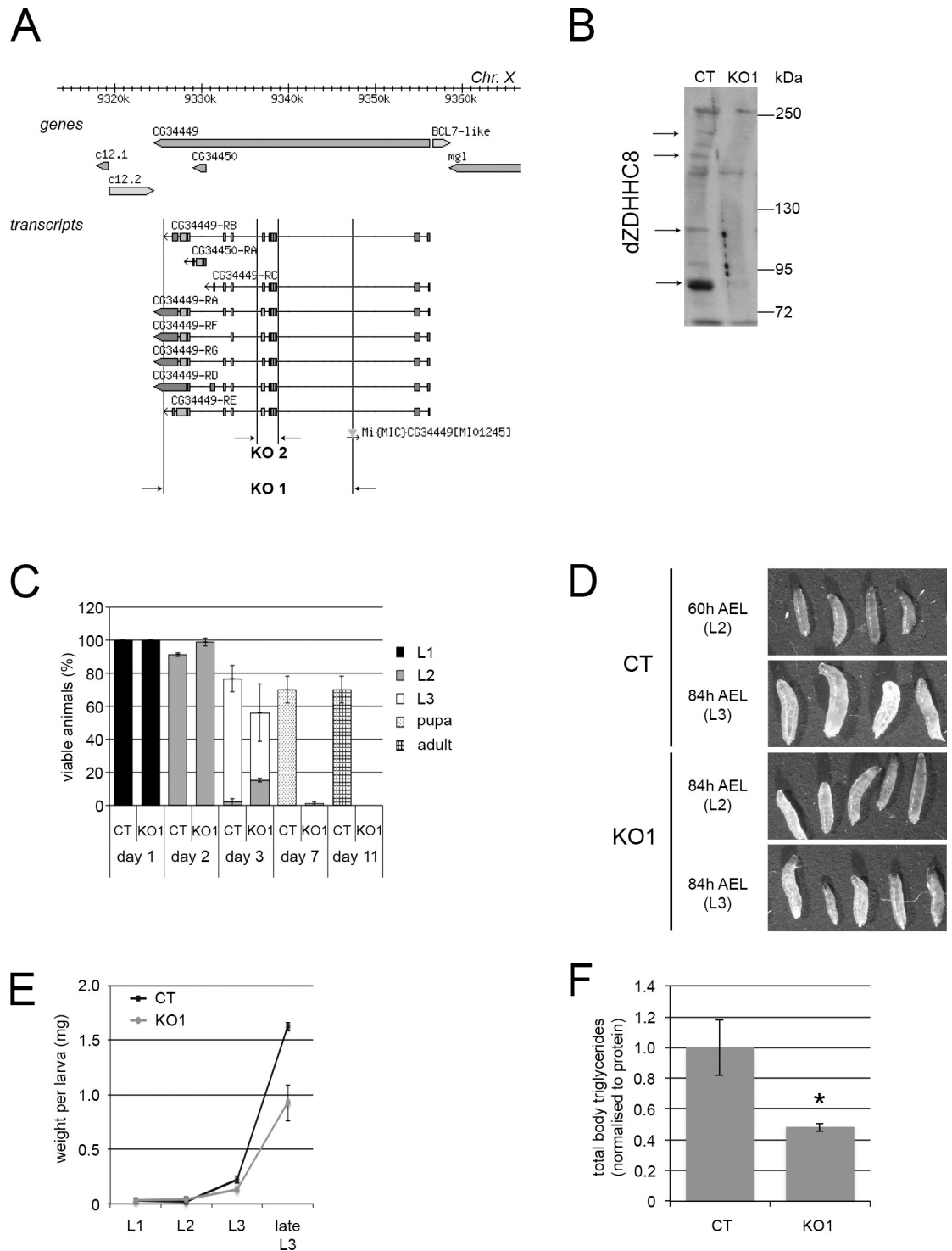


**Fig 2. dZDHHHC8 knockout phenotypes.** (A) Schematic of the dZDHHHC8 genomic locus, indicating transcript isoforms and knockout regions. Two independent dZDHHHC8 knockout lines were generated: knockout 1 (KO1) which removes the majority of dZDHHHC8 as well as CG34450, and knockout 2 (KO2) which removes a small region common to all dZDHHHC8 isoforms including the catalytic domain. (B) dZDHHHC8 knockout larvae do not have dZDHHHC8 protein. dZDHHHC8 protein levels were analysed by immunoblotting extracts from control (CT) or dZDHHHC8 knockout (KO1) larvae, separated on a 6% gel with a dZDHHHC8 specific antibody. dZDHHHC8 appears as multiple high molecular weight bands. Arrows indicate dZDHHHC8 protein absent in KO1. (C) dZDHHHC8 mutants are larval lethal. Control (CT) and dZDHHHC8 knockouts (KO1) were collected as L1 larvae and the number and developmental stage (judged by mouth hook morphology) of viable animals was determined after 1–11

days. KO1 animals start dying at the L2/L3 transition with very few animals reaching pupal stage. Some lethality of control animals is observed in this experiment, due to all animals being picked out of the food and sorted daily for scoring. Error bars = stdev.  $n = 3 \times 60$  L1/genotype. (D) dZDHHC8 phenotypes appear at the L2/L3 transition. Shown are control (CT) and dZDHHC8 mutant (KO1) larvae imaged at 60h after egg laying (AEL) (corresponds to wildtype larval stage 2) or 84h AEL (corresponds to wildtype larval stage 3). The developmental stage of the depicted larvae, judge by the mouth hook morphology is indicated. KO1 larvae are limited in their capability to molt from L2 to L3, either growing bigger for a few days as L2, or molting but never reaching the size of control L3 larvae. (E) dZDHHC8 mutants weigh less than controls. dZDHHC8 knockout larvae (KO1) are lighter than control (CT) larvae with the difference starting at the L2/L3 transition. Error bars = stdev.  $n = 3 \times 20$  larvae/genotype. (F) dZDHHC8 mutants are lean. Shown are total body triglyceride levels, normalized to total body protein, for control (CT) and dZDHHC8 knockout (KO1) L3 larvae. Error bars = stdev.  $n = 3 \times 6$  larvae/genotype. \*  $t$  test = 0.04.

<https://doi.org/10.1371/journal.pone.0198149.g002>

stage of live animals during the following 11 days (Fig 2C). In this and all other experiments, control animals are  $w^{1118}$  animals with the same genetic background as the dZDHHC8<sup>KO1</sup> (see Materials & Methods). This revealed that dZDHHC8<sup>KO1</sup> animals die around the transition from larval stage 2 to 3. This is also true for dZDHHC8<sup>KO2</sup> animals, as well as dZDHHC8<sup>KO1/KO2</sup> transheterozygous animals. Due to the similarity in phenotype of the two alleles, we subsequently characterized in depth allele KO1. Examination of animal morphology showed that dZDHHC8 knockouts have a defect in molting from L2 to L3. Many animals fail to molt, and remain L2 for a few days, continuing to grow to a size larger than normal L2 larvae (Fig 2D). Other dZDHHC8<sup>KO1</sup> larvae molt to L3, but fail to grow and do not reach the size of control animals (Fig 2D, bottom row). Occasionally, we observed dead L3 larvae with their L2 carcass still attached to the mouth hooks. dZDHHC8 knockout animals also have metabolic phenotypes that become apparent at the L2/L3 developmental stage. dZDHHC8<sup>KO1</sup> weigh less and have less total body triglycerides than control animals (Fig 2E and 2F). Unexpectedly, we did not observe tissue overgrowth in dZDHHC8<sup>KO1</sup> animals, but this may be due to differences in tissue-specific versus systemic loss of function, as also observed for other growth regulators (see Discussion). In sum, the data from knockdown and knockout experiments suggest a function of dZDHHC8 in growth and metabolism.

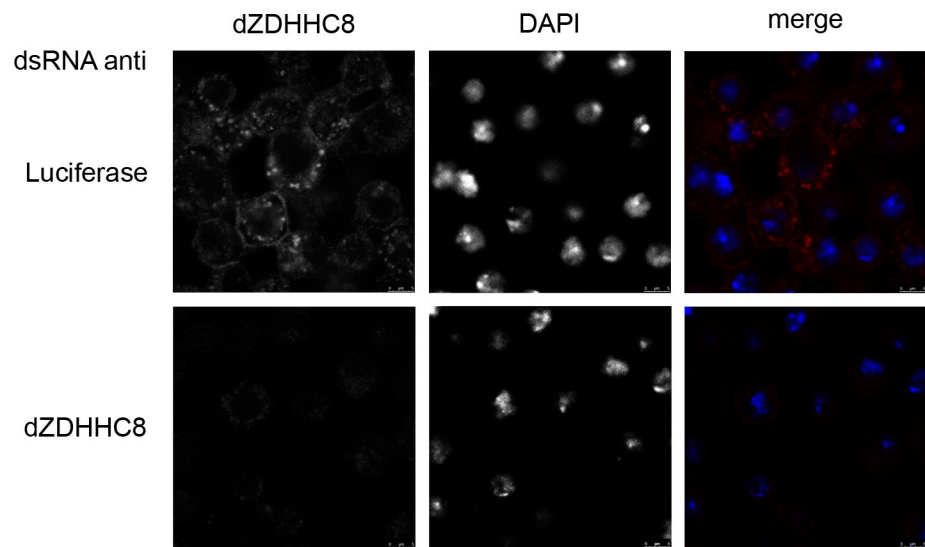
### dZDHHC8 resides at the Golgi and plasma membrane

Palmitoyltransferases such as dZDHHC8 typically localize either to the ER or to the Golgi [17]. To determine the subcellular localization of dZDHHC8 we first tested whether our self-made dZDHHC8 antibody specifically detects endogenous dZDHHC8 by immunostaining. To this end, we stained Drosophila S2 cells that had been treated either with control dsRNA (luciferase dsRNA) or a dsRNA targeting dZDHHC8 (Fig 3A). This revealed a speckled staining in control cells which was absent in dZDHHC8 knockdown cells, suggesting that the antibody is specific for dZDHHC8. In addition to the speckled pattern, some dZDHHC8 also appears to localize to the plasma membrane, in agreement with what has been observed for ZDHHC8 in canine MDCK cells [18]. To figure out whether the speckled appearance is due to dZDHHC8 localization at a specific organelle, we expressed markers for different subcellular compartments in Drosophila S2 cells and co-stained for endogenous dZDHHC8 (Fig 3B). We found that dZDHHC8 co-localizes with a Golgi-tethered protein (Golgi-tethered Fringe-myc [19]) but not with endosomal, ER, or lysosomal markers (Fig 3B).

### Acyl-Biotin exchange (ABE) assay identifies palmitoylated proteins in Drosophila as well as dZDHHC8 targets

To identify proteins that are palmitoylated by dZDHHC8 we used a method called acyl-biotin exchange (ABE). This method allows acyl chains on proteins to be replaced with biotin for streptavidin pull down (Fig 4A). Subsequently, acylated proteins can be identified by mass

A



B

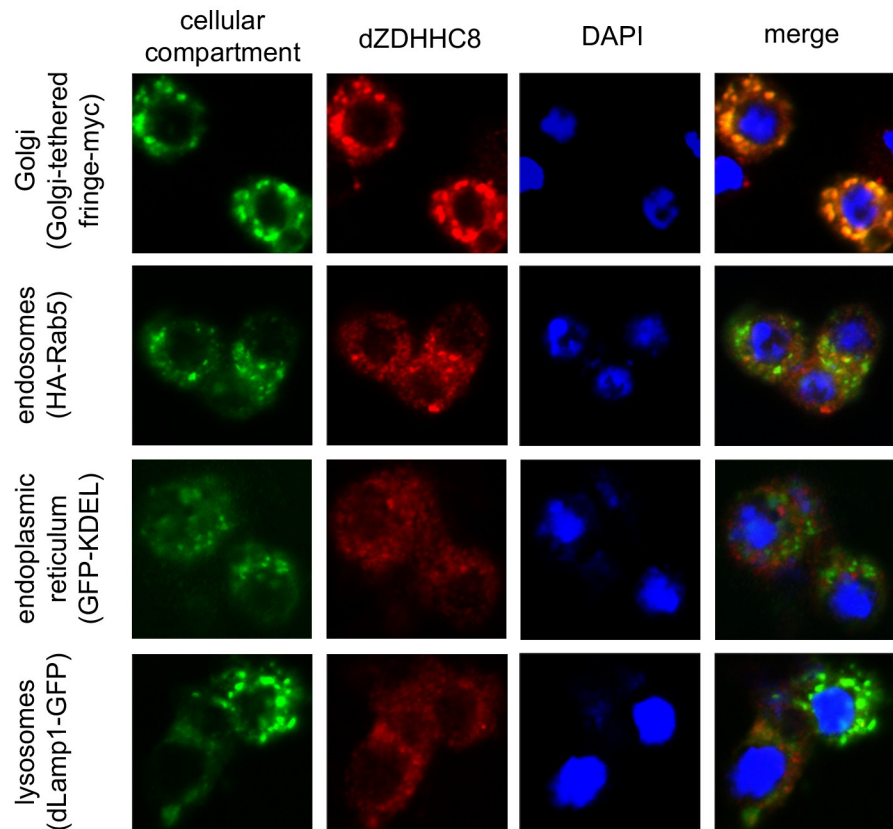


**Fig 3. dZDHHC8 resides at the Golgi.** (A) Antibody against dZDHHC8 specifically detects dZDHHC8 in immunofluorescent stainings of Drosophila S2 cells treated with control (luciferase) dsRNA as there is no staining

upon dZDHC8 knockdown (dsRNA anti dZDHC8). (B) Endogenous dZDHC8 (red) was co-stained with markers for different cellular compartments (green). Overexpressed organelle markers are Golgi-tethered fringe-myc, HA-Rab5 marking endosomes, GFP-KDEL marking endoplasmic reticulum and dLamp1-GFP marking lysosomes. DAPI was used to stain nuclei. dZDHC8 co-localises with the Golgi-tethered marker.

<https://doi.org/10.1371/journal.pone.0198149.g003>

spectrometry (ABE-MS) or western blotting (ABE-WB, Fig 4A). As a negative control, the hydroxyl-amine ( $H_3NO$ ) is omitted, and acylated proteins are the ones observed differentially represented in the  $+H_3NO$  pulldown compared to the  $-H_3NO$  pulldown. We performed ABE-MS from lysates of control and dZDHC8 knockout animals. Three independent experiments yielded a list of 159 genes that are significantly acylated in either the control or knockout animals or both (S1 Table,  $FDR < 0.1$ ). This provides a list of proteins that are acylated (e.g. palmitoylated, stearylated, or myristoylated) in *Drosophila* and may constitute a useful resource for the community. Amongst these proteins are proteins previously known to be palmitoylated in mammals such as Flotilin 1 (Flo1) and Flotilin 2 (Flo2) or cysteine string protein (Csp). We further validated our mass spectrometry data by performing ABE-WB on lysates of larvae overexpressing HA-tagged Csp and Ras64B and confirmed that Csp and Ras64B are palmitoylated in *Drosophila* (Fig 4B). From the relative ratio of the proteins detected in the ABE pulldown compared to the lysate input (lanes 3 vs 1 in Fig 4B), it appears that Ras64B is acylated at very low stoichiometry. Indeed a method similar to the ABE method whereby the acylation is replaced with a polyethylene glycol (PEG) molecule of defined mass, termed acyl-PEG exchange (APE) [20], revealed an up-shifted band for Csp but no detectable up-shifted band for Ras64B (Fig 4C). Since the methodologies of the ABE and APE assays are very similar, we conclude that only a small fraction of Ras64B is acylated and can be detected using the ABE assay (Fig 4B and Fig 5 below) which starts with large sample amounts and enriches for acylated proteins by pulldown.

To identify dZDHC8 targets we screened our ABE-MS data for proteins that are less palmitoylated in the dZDHC8<sup>KO1</sup> samples compared to the control samples (S2 Table). Using a cutoff of a 40% decrease in palmitoylation in KO compared to control, we identified 13 proteins as potential targets of dZDHC8, however the difference in control vs KO was not statistically significant.

To link the dZDHC8 loss of function fly phenotype to a dZDHC8 target protein we initially focused on scribble because of its known tumor suppressor function. First, we performed ABE-WB of endogenous scribble from control and knockout larvae. We found that scribble is palmitoylated at least in part by dZDHC8 as there is less palmitoylated scribble pulled down in knockout animals compared to control animals (Fig 4D, compare KO1  $+H_3NO$  to CT  $+H_3NO$ ). This suggests that even though the mass spectrometry analysis did not yield statistically significant differences between control and dZDHC8<sup>KO1</sup> samples, the data can still be used as a list of potential dZDHC8 targets.

We hypothesized that impaired palmitoylation of scribble could lead to changes in scribble activity, which we tested in three different ways: (1) To test if dZDHC8 lethality was due to impaired scribble activity we tested whether removing one copy of scribble in a dZDHC8<sup>KO1/+</sup> heterozygous mutant background would lead to synthetic lethality. However, dZDHC8<sup>KO1/+</sup>, scribble<sup>-/+</sup> transheterozygous mutants were as viable as their control counterparts (in a cross with 149 analyzed progeny, dZDHC8<sup>KO1/+</sup>, scribble<sup>-/+</sup> females survived at 86% the expected mendelian ratio). (2) Scribble regulates cell polarity in a protein complex with lethal giant larvae (Lgl) and discs large (Dlg), and follicle cells lacking scribble are rounded and often multilayered [21]. To examine whether dZDHC8 loss-of-function leads to defects in follicle cell polarity we stained dZDHC8 mutant follicle clones for Dlg (S4A Fig). However, follicle cells lacking

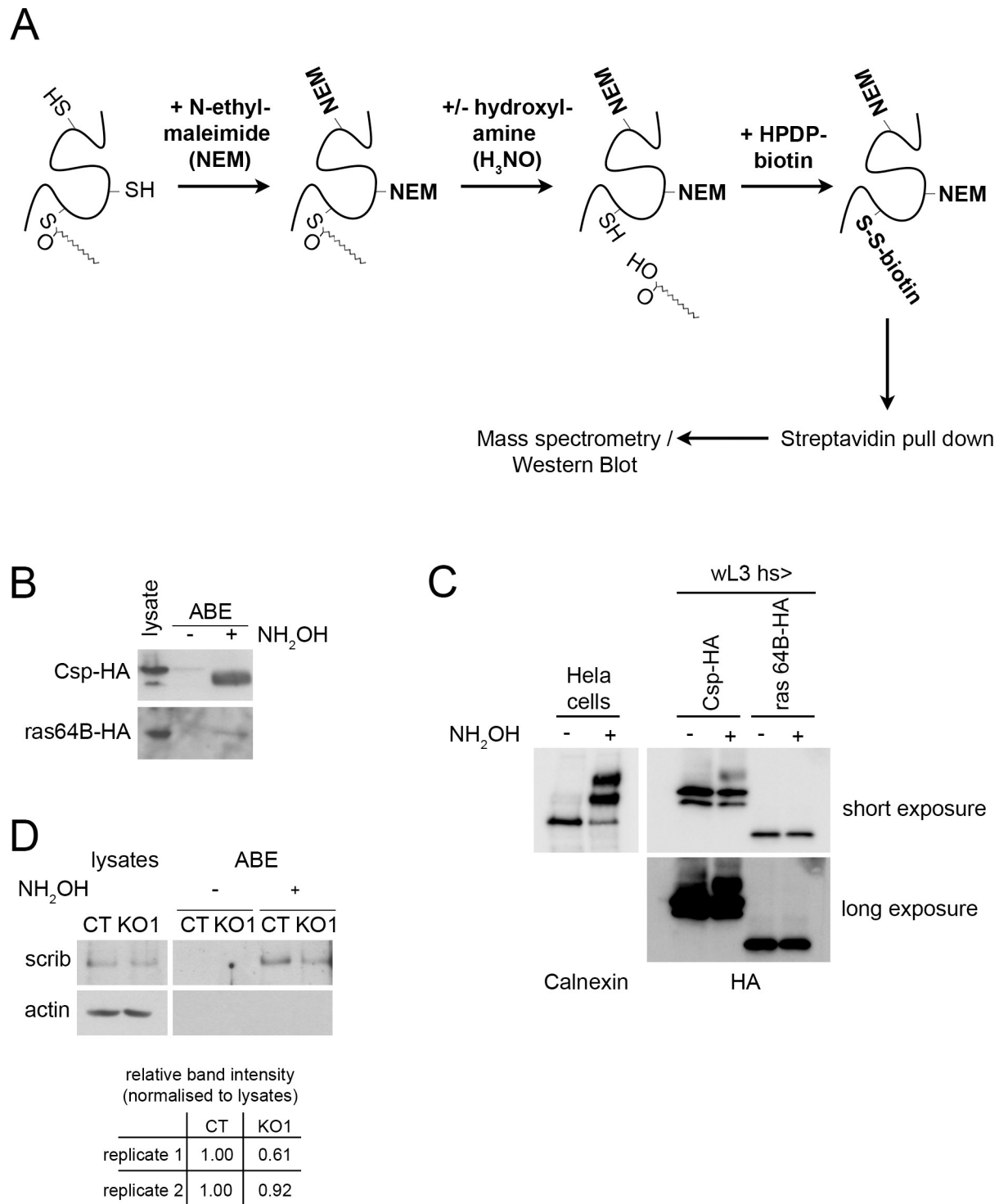


**Fig 4. Acyl-Biotin Exchange (ABE) assay identifies acylated proteins in Drosophila as well as potential dZDHH8 targets.** (A) Schematic representation of an Acyl-Biotin Exchange (ABE) assay followed by mass spectrometry (ABE-MS) to identify acylated proteins (ie palmitoylated, stearoylated, etc). First, lysates are treated with N-ethylmaleimide to block free cysteine-residues on proteins. Acylation on proteins is then removed by hydroxylamine ( $H_3NO$ ) treatment yielding free cysteines that were previously acylated. Free cysteines subsequently react with thiol-reactive HPDP-biotin and biotinylated proteins are pulled down with streptavidin-beads. Eluted proteins are analysed by mass spectrometry or western blot (ABE-WB). Every ABE-assay includes a non- $H_3NO$  treated control to distinguish acylated proteins from unspecifically biotinylated proteins. (B) Csp and Ras64B are acylated. ABE assay was performed on lysates from L3 larvae expressing HA-tagged Csp or Ras64B under the control of heatshock-Gal4 24h after heatshock. Csp and Ras64B are acylated as they are

specifically pulled down in the H<sub>3</sub>NO treated, but not in H<sub>3</sub>NO untreated control samples. (C) The stoichiometry of ras64B acylation is very low, in agreement with panel (B), as it cannot be detected by the acyl-PEG exchange (APE) method [20]. Detection of calnexin acylation in HeLa cells and of Csp acylation in larvae serve as positive controls for the method. (D) Scrib is palmitoylated, partly by dZDHHHC8. Shown are endogenous scrib protein levels from control (CT) and dZDHHHC8 knockout (KO1) larvae in lysates and after ABE assay. Scrib is detected after ABE in H<sub>3</sub>NO treated samples of CT and to a lesser extent of KO1 larvae, but not in control samples (-H<sub>3</sub>NO).

<https://doi.org/10.1371/journal.pone.0198149.g004>

dZDHHHC8 appeared morphologically normal as a monolayer and we could not observe any differences in Dlg subcellular localization in dZDHHHC8 knockout clones compared to neighboring cells (S4A Fig). (3) Scribble also affects Hippo signaling [22]. We tested whether the activity of Yorkie, a transcriptional co-activator downstream of Hippo was affected using the transcriptional reporter expanded-lacZ (ex-lacZ). We generated dZDHHHC8 knockout clones in the wing disc carrying ex-lacZ and immuno-stained them with an antibody against  $\beta$ -galactosidase (S4B Fig). Again, we did not see any differences in expanded expression in knockout clones compared to neighboring wildtype cells (S4B Fig). Even though dZDHHHC8 seems to palmitoylate scribble, we could not find evidence that the degree of drop in scribble palmitoylation caused by dZDHHHC8 loss is sufficient to affect scribble activity. Therefore, we focused on a different target of dZDHHHC8.

### dZDHHHC8 affects Ras64B stability

Looking at the list of potential dZDHHHC8 targets our attention was caught by Ras64B because ras proteins are known to play a role in growth control. We looked for genetic interaction of dZDHHHC8 and Ras64B and found that overexpression of Ras64B enhances dZDHHHC8 mutant lethality (Fig 5A). To verify our ABE-MS data we performed an ABE-WB assay from larval lysates of Ras64B-HA overexpressing control and dZDHHHC8 knockout animals (Fig 5B). We found that knockout animals have indeed less palmitoylated Ras64B (Fig 5B, ABE KO1 + H<sub>3</sub>NO versus ABE CT + H<sub>3</sub>NO) however total Ras64B protein was also decreased (Fig 5B, first two lanes). This suggests that loss of dZDHHHC8 either leads to reduced Ras64B palmitoylation and, as a consequence, reduced Ras64B stability, or the other way around—that dZDHHHC8 affects Ras64B stability, and as a consequence palmitoylation. We therefore studied the effects of dZDHHHC8 on Ras64B stability and palmitoylation. We tested whether dZDHHHC8 loss of function leads to decreased Ras64B stability by expressing Ras64B-HA in control and dZDHHHC8<sup>KO1</sup> animals (Fig 5C). We used a heat-inducible driver (hs>Ras64B) and looked at Ras64B-HA protein levels at different time points after heat-shock. This showed that Ras64B-HA stability is strongly dependent on dZDHHHC8 with Ras64B-HA protein levels being decreased in dZDHHHC8 knockout animals even when Ras64B-HA is expressed at low levels without any heat-shock (Fig 5C, 0h post hs). Ras64B has five cysteines that could serve as potential palmitoylation sites. Two cysteines belong to the c-terminal CAAX motif (CCLM amino acids 189–192), which is required for ras farnesylation, which in turn serves as a priming event for ras palmitoylation [23]. As expected, mutation of cysteines in the CAAX motif resulted in a complete loss of Ras64B palmitoylation (Fig 5G). To test whether any of the other three cysteines is palmitoylated we mutated each of them to alanine and performed ABE-WB on lysates of larvae expressing Ras64B wildtype (WT) or Ras64B alanine mutants (C46A, C120A, C147A, Fig 5D). To our surprise, each of the alanine mutant versions is less palmitoylated compared to WT Ras64B (compare +H<sub>3</sub>NO lanes, Fig 5D) yet each mutant is still palmitoylated (compare + to—H<sub>3</sub>NO for each mutant). This suggests that Ras64B is palmitoylated on more than one site. Therefore, we mutated two cysteines at the same time (Fig 5E) and found that again palmitoylation is present in each of the three double-mutants (Fig 5E), suggesting that all three sites are palmitoylated. In agreement with this, simultaneous mutation of

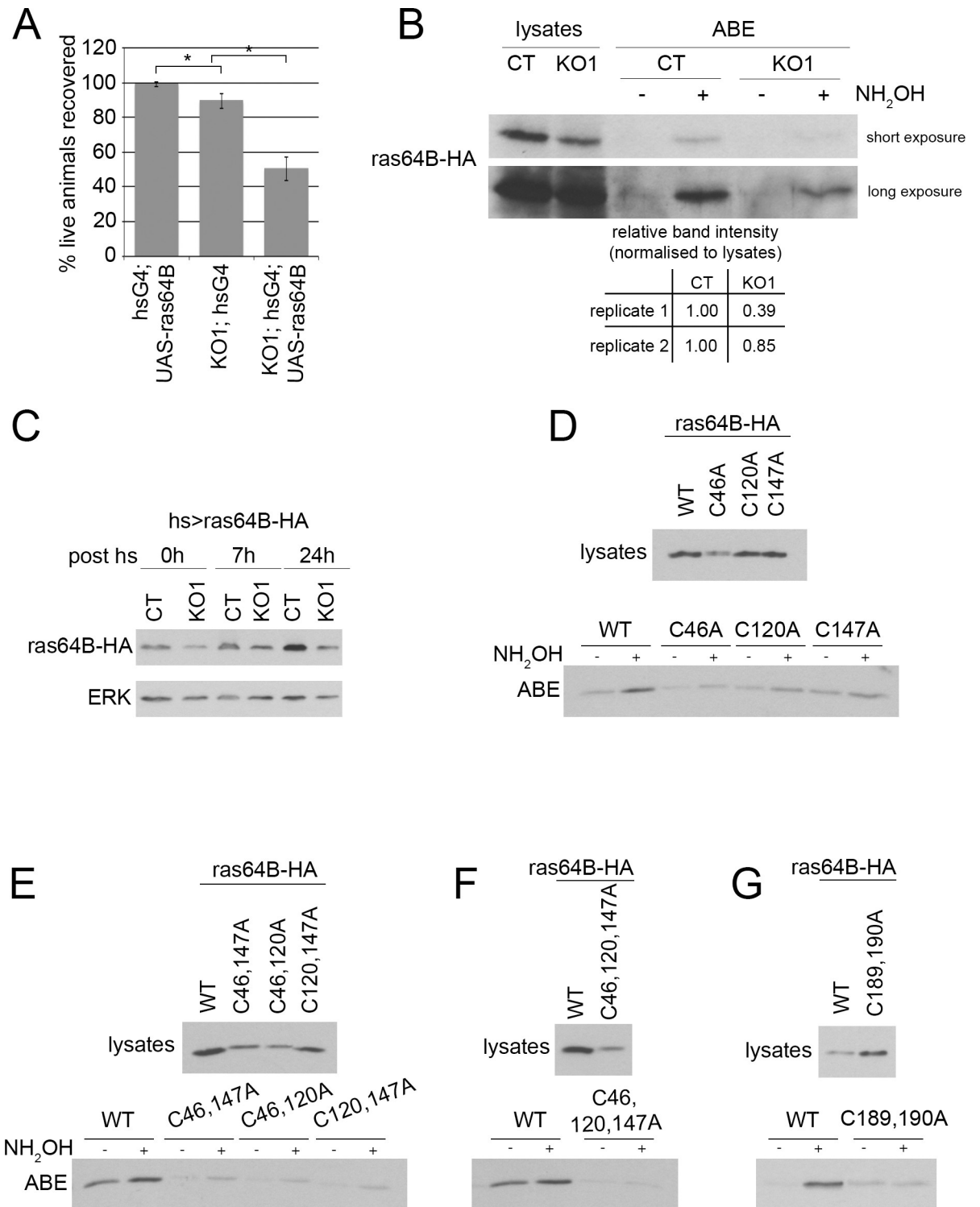


**Fig 5. dZDHHC8 affects Ras64B stability.** (A) Ras64B overexpression decreases viability of dZDHHC8 knockouts. Four days after L1 collection, the number of live Ras64B overexpressing larvae (hsG4; UAS-Ras64B), dZDHHC8 homozygous mutant larvae (KO1; hsG4) or larvae overexpressing Ras64B in dZDHHC8<sup>KO1</sup> mutant background (KO1; hsG4; UAS-Ras64B) was determined. Ras64B overexpression in the dZDHHC8<sup>KO1</sup> mutant background causes synergistic lethality. Error bars = stdev. n = 3x60 larvae/genotype. \* ttest ≤ 0.04. (B) ABE assay was performed on lysates from control (CT) and dZDHHC8 knockout (KO1) early L3 larvae expressing Ras64B under the control of heatshock-Gal4 24h after heatshock. KO1 larvae have less palmitoylated Ras64B-HA when compared to WT controls but also less total Ras64B-HA protein. (C) dZDHHC8 affects Ras64B stability. Protein levels of Ras64B-HA expressed with hsG4 in control (CT) and

dZDHHC8 knockout (KO1) larvae were assayed by immunoblotting at different time points after heat-shock. ERK was used as a loading control. KO1 larvae have less Ras64B-HA protein than CT larvae at any time point. (D) Ras64B is palmitoylated on at least two cysteines. Larvae expressing HA-tagged wildtype Ras64B, or mutant Ras64B where each of the three cysteine residues present in Ras64B is mutated to alanine. All expression constructs are inserted in the same genomic locus using phiC31-directed integration, and their expression induced using hsG4 and collecting samples for ABE 24h after heat-shock. All Ras64B-HA C/A mutants are still palmitoylated, albeit less than WT Ras64B-HA. Note that Ras64B C46A protein levels are lower than wildtype Ras64B. (E-G) Ras64B is palmitoylated on all three cysteines C46, C120, C147. Assay performed as in (B). Each of the Ras64B-HA double cysteine mutants is still palmitoylated (E). Only mutating all three cysteines at the same time (F) or mutating the cysteine before and within the CAAX motif (G) abolishes palmitoylation. Note that protein levels of Ras64B versions carrying C46A are lower.

<https://doi.org/10.1371/journal.pone.0198149.g005>

all three cysteines to alanine completely abolished palmitoylation of Ras64B (Fig 5F). In sum, Ras64B is palmitoylated on Cys46, Cys120 and Cys147.

Studying the various Ras64B mutants we realized that whenever Cys46 is mutated to alanine (Fig 5D–5F, C46A) Ras64B protein levels strongly drop in the lysates, just like they do when WT Ras64B is expressed in dZDHHC8 mutants (Fig 5B). This suggests that Cys46 plays a role in Ras64B protein stability. Until now, however, it is unclear whether dZDHHC8 palmitoylates Ras64B at Cys46 thereby regulating its stability, or whether dZDHHC8 affects Ras64B stability indirectly through some other mechanism.

## Discussion

The function of hZDHHC8 has been mainly characterized to date in the brain, where loss of the genomic hZDHHC8 locus in microdeletions at 22q11 is associated with cognitive deficits and schizophrenia [24–26]. To our knowledge, hZDHHC8 has not been implicated in cancer so far, except that knockdown of hZDHHC8 makes mesothelioma cells more sensitive to radiotherapy [27]. We report here the functional characterization of the Drosophila ortholog of hZDHHC8, CG34449/dZDHHC8. Knockdown of dZDHHC8 in the Drosophila wing resulted in tissue overgrowth due to increased cell proliferation (Fig 1) suggesting that dZDHHC8 inhibits cell proliferation tissue autonomously. When we generated knockout flies, we found that dZDHHC8 mutant flies are small and lean and die as larvae (Fig 2). The lethality may be the result of loss of palmitoylation on all dZDHHC8 targets and is therefore very pleiotropic. The fact that mild knockdown results in tissue overgrowth whereas complete loss of function is lethal has been reported also for other genes, as for instance TSC2 loss of function clones in the eye cause overgrowth whereas ubiquitous loss of function of TSC2 is embryonic lethal [28].

In their characterization of palmitoyltransferases and thioesterases, Bannan and colleagues previously showed that most of Drosophila palmitoyltransferases localize to the ER or Golgi [17]. Our findings complement their findings by showing that also dZDHHC8 localizes to the Golgi (Fig 3). Furthermore, we identify here palmitoylated proteins on a proteome wide level in Drosophila by performing ABE assays from larvae. This yields a list of 159 acylated target proteins (S1 Table) which will hopefully constitute a useful resource for the community.

Comparing palmitoylated proteins of control and dZDHHC8 mutant larvae we find scribble to be palmitoylated in part by dZDHHC8. Scribble palmitoylation is decreased in dZDHHC8 mutants, however not completely abolished (Fig 4). This suggests that there is another palmitoyltransferase acting on scribble. Potentially, this could be the fly homologue of ZDHHC7, as human ZDHHC7 has been shown to palmitoylate scribble in HEK293A cells [29]. In addition to scribble, we also verified Ras64B as a target of dZDHHC8 (Fig 5). We find that dZDHHC8 lethality is enhanced by overexpression of Ras64B suggesting that they act synergistically (Fig 5A). The mechanism appears rather complicated as loss of dZDHHC8 leads to destabilization of Ras64B. It has been proposed for other proteins that lack of palmitoylation

can lead to their destabilization [30,31]. In this case here it is unclear whether Ras64B destabilization is due to impaired palmitoylation or whether dZDHHC8 acts on Ras64B in a different manner to affect its stability, and as a consequence we also see reduced palmitoylation. It has been reported that overexpression of Ras64B in the wing causes the formation extra vein material [32]. Interestingly, we find that knockdown of dZDHHC8 also leads to ectopic veins (Fig 1D) again pointing towards dZDHHC8 acting on Ras64B.

Generally, we have found it difficult to attribute the loss-of-function phenotypes for the dZDHHC8 transferase to individual downstream targets. This might be because ZDHHC8 palmitoylates multiple target proteins, yielding a combined phenotype, with each individual target contributing only partially to the combined phenotype. In addition, redundancy between ZDHHC8 and other ZDHHC transferases may cause the function of individual targets to be only mildly impaired in the absence of ZDHHC8. Finally, genetic interactions were made difficult by the fact that both Ras64B and Scribble are required for viability. Hence, in sum, we do not know which ZDHHC8 targets are responsible for the lethality of ZDHHC8 knockouts.

We find that knockdown of dZDHHC8 causes tissue overgrowth, which is a cancer-relevant phenotype. Furthermore, we provide data suggesting that scribble and Ras64B are targets of Drosophila ZDHHC8. These findings possibly shed some light on the epidemiological links between hZDHHC8 and cancer (S1 Fig). Admittedly, the relationship between hZDHHC8 and cancer progression is complex, because in some cases elevated ZDHHC8 expression correlates with poor prognosis, and in some cases it correlates with good prognosis (S1 Fig). Hence significant more work will be required to understand this relationship. Nonetheless, the fact that dZDHHC8 knockdown causes a cancer-relevant phenotype in Drosophila suggests it may be worthwhile looking at hZDHHC8 more closely.

## Materials & methods

### Plasmids and fly strains

The plasmids used in the study are listed in S3 Table. Full sequences can be obtained upon request. Sequences of oligos are in S4 Table. *apterous-Gal4*, *engrailed-Gal4*, *tubulin-Gal4*, *heat-shock-Gal4*, *UAS-GFP*, *Mi{MIC}dZDHHC8<sup>MI01245</sup>*, *UAS-ras64B RNAi* (stock 29318), and *hsFlp*, *hs-SceI/Cyo*, *y,w*, *nos-phiC31(X)*; *Sco/Cyo* (stock 34770) were obtained from Bloomington Stock Center. *UAS-dZDHHC8 RNAi* lines GD5521 (#1) and GD48025 (#2) were obtained from Vienna Drosophila Research Center. From DGRC we obtained expression constructs for *Csp-HA* (clone UFO08205) and *ras64B-HA* (clone UFO6356). For expression of tagged *ras64B* in Drosophila, plasmids pKH410, 411, 412, 413, 414, 430, 433, 434 and 437 (S3 Table) were injected into vk33 (Bloomington stock 32543) flies to allow site directed insertion on the third chromosome. The dZDHHC8 RNAi #3 line was generated by injecting pKH364 into *w<sup>1118</sup>* flies. pKH364 is a pWIZ construct containing dZDHHC8 genomic sequence amplified by PCR using the oligos OKH528/529. Flag-tagged dZDHHC8 was generated by cloning the dZDHHC8 coding sequence amplified using OKH402/407 into the pMT>Flag vector (pKH295). Scribble-HA expression construct was made by subcloning the scribble coding sequence from DGRC clone RE02389 into the pMT vector (pKH402).

### dZDHHC8 knockout generation

dZDHHC8 knockout 1 was generated using the MIMIC line *Mi{MIC}dZDHHC8<sup>MI01245</sup>*, in which the MIMIC cassette flanked by attP sites was replaced by Recombination Mediated Cassette Exchange (RMCE) with a knockout cassette flanked by attB sites [33]. The knockout cassette consisted of a yellow marker gene, followed by a *SceI* restriction site, a sequence

homologues to the genomic region downstream of the knockout locus and a mini white gene (pKH304). RMCE was achieved by injecting pKH304 (S3 Table) into F1 embryos of nos-phiC31 x Mi{MIC}dZDHC8<sup>M101245</sup> and screening for w+, y+ knockout donors. The correct orientation of the knockout cassette in the donor line was verified by PCR. The donor line was subsequently crossed to hs-SceI, and SceI expression was induced by heat-shocking the F1 on day 2 for 1h at 37°C. 600 F1 virgins that were w+ and mosaic for yellow were crossed to balancer males and the F1 was screened for w+, y- progeny. In those animals the double-strand break induced by SceI restriction had been repaired by homologous recombination using the genomic sequence of the knockout cassette. This led to loss of the yellow marker gene. We recovered 1 female from all progeny of the 600 crosses. dZDHC8 knockout 2 was generated by homologous recombination as described previously [34] using pKH261 as a donor vector.

### Back-crossing of dZDHC8 mutants

To clean the genetic background of dZDHC8 mutants, heterozygous virgin females carrying the dZDHC8<sup>KO</sup> allele were back-crossed to w<sup>1118</sup> males for 4 generations. In parallel FM7 balancer virgins were back-crossed to w<sup>1118</sup> males to place the FM7 balancer into the w<sup>1118</sup> genetic background. After four rounds of back-crossing, single heterozygous knockout virgins were crossed to single FM7 males to establish stocks. Unless indicated otherwise w<sup>1118</sup> was used as the control strain throughout all experiments.

### Cell culture knockdowns and quantitative RT-PCR

dsRNAs were made using oligos OKH385/386 (anti CG34450, S2 Fig), OKH394/395 (anti CG34449, Fig 3A). S2 cells seeded in 6 well plates at 3x10<sup>6</sup> cells/well/ml were treated with 12μg dsRNA in serum-free medium for 1h before 2ml of Schneider's medium (GIBCO 21720) containing 10% FBS was added. After 5 days of knockdown cells were lysed and processed for SDS-PAGE and western blotting. Quantitative RT-PCR was performed using Maxima H Minus Reverse Transcriptase (Thermo Scientific EP0752), Maxima SYBG/ROX qPCR Master mix (Thermo Scientific K0223) and oligos OKH383/384 (PCR A, S3 Fig), OKH375/376 (PCR B, S3 Fig), OKH371/372 (PCR C, S3 Fig). Oligo sequences can be found in S4 Table.

### Stainings and antibodies

Immunostainings of cells or wing discs were performed as described previously [35]. Antibody against dZDHC8 was raised in guinea pigs immunized with protein expressed in E. coli from pKH276 (used for immunostainings) or pKH278 (used for western blots). Other antibodies used were rat anti HA-tag (clone 3F10, Roche, 11 867 423 001), mouse anti actin (Hybridoma Bank, JLA20), mouse anti β-Galactosidase (Promega, Z378A), rabbit anti GFP (Torrey Pines Biolab TP401), rabbit anti scribble (kind gift from David Bilder), rabbit anti ERK1 (Cell Signaling 4695).

### Triglyceride measurements

Triglyceride levels were measured in L3 larvae as described previously [35].

### Clone size and wing measurements

GFP marked dZDHC8 knockout clones and lacZ marked twin clones were generated by heat-shocking FRT18, GFP, KO/FRT18, lacZ female larvae for 45 min at 37°C three days prior wandering. Wing discs were stained with anti-GFP and anti-β-Galactosidase antibodies and imaged a Leica SP8 confocal system with a 40x objective. Adult wings were imaged using an

epifluorescent microscope with a 2.5x or 10x (for trichome density) objective. Clone size, wing compartment area as well as area of ectopic vein material were measured with ImageJ polygon selection tool.

### Acyl-biotinyl-exchange (ABE) assay

Expression of UAS-constructs was induced 24h prior to lysis by a 45min heat-shock at 37°C. The ABE assay was performed as described in [36]: Circa 160 L2 larvae were homogenised with a plastic pistil in 1.2ml lysis buffer containing 1.7% Triton X-100, 10mM N-ethylmaleimide (NEM), 2x proteinase inhibitor cocktail and 2mM PMSF and lysed for 15min on ice. After tissues were spun down, as an input sample 40µl lysate were mixed with 10µl 5x Lämmli and subsequently boiled for 5min at 95°C. Differing from the protocol published by Wan et al. [36] biotinylated proteins were finally pulled down using 15µl slurry of streptavidin coupled, magnetic dyna beads (Invitrogen 65001) and eluted in 30µl elution buffer. After elution samples were mixed with 15µl 5x Lämmli and boiled for 5min at 95°C.

### Acyl-PEG exchange (APE) assay

The APE assay was performed as described in [20]. To obtain lysates of roughly 2mg/ml, 5 wandering larvae were lysed in 400µl lysis buffer or 10<sup>6</sup> Hela cells were lysed in 230µl lysis buffer. S2 cells were transfected in 6-well plates with pMT>scrib-HA +/- pMT>FLAG-dZDHHC8 for 24h, then induced for 24h with Cu<sup>2+</sup>, and then, having reached 80% confluence, lysed in 200µl lysis buffer.

### Staining of cellular compartment

The following constructs were expressed in S2 cells to mark cellular organelles: pMT-GFP-KDEL marking endoplasmic reticulum, pMT-myc-fringe Golgi-tethered, pUAS-HA-Rab5 marking endosomes, pMT-dLamp1-GFP marking lysosomes.

### Supporting information

**S1 Fig. CG34449 is the Drosophila ortholog of human ZDHHC8.** (A) ZDHHC8 expression levels correlate with increased or reduced cancer survival depending on cancer type. Kaplan-Meier plots (best separation, taken from The Human Protein Atlas using data from The Cancer Genome Atlas <https://cancergenome.nih.gov>) show a correlation between ZDHHC8 expression and patient survival for different cancer types. In renal (log-rank P value 4.04 x 10<sup>-4</sup>) and cervical cancer (log-rank P value 9.68 x 10<sup>-4</sup>) high ZDHHC8 expression correlates with decreased survival, whereas in lung (log-rank P value 1.03 x 10<sup>-2</sup>) and pancreatic cancer (log-rank P value 9.34 x 10<sup>-3</sup>) low ZDHHC8 expression correlates with decreased survival. (B) BLAST search using the Flybase BLAST server [37] of the Drosophila proteome using the protein sequence of human ZDHHC8 (NCBI Reference Sequence NP\_037505.1) yields CG34449 as the top hit, with an E value of 10<sup>-76</sup>. Conversely, BLASTing the protein sequence of Drosophila CG34449 against the human proteome yields ZDHHC8 as the top hit with an E value of 10<sup>-87</sup>, identifying ZDHHC8 as the human orthologue of Drosophila CG34449. (TIF)

**S2 Fig. dZDHHC8 knockdown efficiency is quite good in the wing disc.** (A) Wing discs with dZDHHC8 knockdown in the dorsal compartment using apterous-GAL4 (apG4), stained anti dZDHHC8. (B) Expression of dZDHHC8 RNAi in the posterior compartment of the wing using engrailed-Gal4 (en>dZDHHC8 RNAi #1) at 29°C causes an increase in posterior compartment size normalized to anterior when compared to control wings (enG4>+). Error

bars = stdev.  $n = 10$ . \*\*\*  $t$ test =  $1 \times 10^{-4}$ . (C) Expression of dZDHC8 RNAi in the posterior compartment of the wing using hedgehog-Gal4 ( $hh > dZDHC8$  RNAi #1) causes an increase in posterior compartment size normalized to anterior when compared to control wings ( $enG4 > +$ ). Error bars = stdev.  $n = 10$ . \*\*\*  $t$ test =  $1 \times 10^{-3}$ . (D) Representative examples of wings used to quantify cell size in Main 1C. Quantified regions are marked with a yellow box, and shown in higher magnification underneath.

(TIF)

**S3 Fig. dZDHC8 and CG34450 are transcriptionally linked.** The expression of different dZDHC8 exons (PCR B and C) was analysed by quantitative RT-PCR in control cells (dark grey bars) or cells with a CG34450 knockdown (light grey bars). When CG34450 is knocked down, transcript levels of dZDHC8 also decrease suggesting dZDHC8 and CG34450 are not separate genes.

(TIF)

**S4 Fig. Scribble activity in dZDHC8 mutant clones.** (A) dZDHC8 mutant follicle clones (GFP negative) were stained with an antibody detecting endogenous Dlg (red). Dlg localization is not affected in dZDHC8 mutant clones. (B) Three day old dZDHC8 knockout clones (GFP negative) in the wing disc were stained for the yorkie reporter *ex-lacZ* (red). Yorkie activity is not affected in dZDHC8 mutant clones.

(TIF)

**S1 Table. List of acylated proteins in Drosophila.**

(XLSX)

**S2 Table. List of dZDHC8 targets.**

(XLSX)

**S3 Table. List of plasmids used in this study.**

(XLSX)

**S4 Table. List of oligos used in this study.**

(XLSX)

## Acknowledgments

We thank the DKFZ Mass Spectrometry Core facility for mass spec. analyses, Marilena Lutz for technical help, and Natalia Becker from the DKFZ Biostatistics department for help with analyzing the mass spec data. Anti-actin antibody was obtained from the Developmental Studies Hybridoma Bank developed under the auspices of the NICHD and maintained by The University of Iowa.

## Author Contributions

**Conceptualization:** Katrin Strassburger, Aurelio A. Teleman.

**Formal analysis:** Katrin Strassburger, Aurelio A. Teleman.

**Funding acquisition:** Aurelio A. Teleman.

**Investigation:** Katrin Strassburger, Evangeline Kang.

**Methodology:** Katrin Strassburger.

**Supervision:** Aurelio A. Teleman.

**Writing – original draft:** Katrin Strassburger.

**Writing – review & editing:** Aurelio A. Teleman.

## References

1. Aicart-Ramos C, Valero RA, Rodriguez-Crespo I. Protein palmitoylation and subcellular trafficking. *Biochimica et biophysica acta*. 2011; 1808(12):2981–94. Epub 2011/08/09. <https://doi.org/10.1016/j.bbamem.2011.07.009> PMID: 21819967.
2. Mitchell DA, Vasudevan A, Linder ME, Deschenes RJ. Protein palmitoylation by a family of DHHC protein S-acyltransferases. *Journal of lipid research*. 2006; 47(6):1118–27. Epub 2006/04/04. <https://doi.org/10.1194/jlr.R600007-JLR200> PMID: 16582420.
3. Smotrys JE, Linder ME. Palmitoylation of intracellular signaling proteins: regulation and function. *Annual review of biochemistry*. 2004; 73:559–87. Epub 2004/06/11. <https://doi.org/10.1146/annurev.biochem.73.011303.073954> PMID: 15189153.
4. Sanders SS, Martin DD, Butland SL, Lavallee-Adam M, Calzolari D, Kay C, et al. Curation of the Mammalian Palmitoylome Indicates a Pivotal Role for Palmitoylation in Diseases and Disorders of the Nervous System and Cancers. *PLoS Comput Biol*. 2015; 11(8):e1004405. Epub 2015/08/15. <https://doi.org/10.1371/journal.pcbi.1004405> PMID: 26275289; PubMed Central PMCID: PMC4537140.
5. Mansouri MR, Marklund L, Gustavsson P, Davey E, Carlsson B, Larsson C, et al. Loss of ZDHC15 expression in a woman with a balanced translocation t(X;15)(q13.3;cen) and severe mental retardation. *Eur J Hum Genet*. 2005; 13(8):970–7. Epub 2005/05/26. <https://doi.org/10.1038/sj.ejhg.5201445> PMID: 15915161.
6. Mukai J, Liu H, Burt RA, Swor DE, Lai WS, Karayiorgou M, et al. Evidence that the gene encoding ZDHC8 contributes to the risk of schizophrenia. *Nature genetics*. 2004; 36(7):725–31. Epub 2004/06/09. <https://doi.org/10.1038/ng1375> PMID: 15184899.
7. Zhang J, Planey SL, Ceballos C, Stevens SM Jr., Keay SK, Zacharias DA. Identification of CKAP4/p63 as a major substrate of the palmitoyl acyltransferase DHHC2, a putative tumor suppressor, using a novel proteomics method. *Molecular & cellular proteomics: MCP*. 2008; 7(7):1378–88. Epub 2008/02/26. <https://doi.org/10.1074/mcp.M800069-MCP200> PMID: 18296695; PubMed Central PMCID: PMC2493380.
8. Yamamoto Y, Chochi Y, Matsuyama H, Eguchi S, Kawauchi S, Furuya T, et al. Gain of 5p15.33 is associated with progression of bladder cancer. *Oncology*. 2007; 72(1–2):132–8. Epub 2007/11/21. <https://doi.org/10.1159/000111132> PMID: 18025801.
9. Mansilla F, Birkenkamp-Demtroder K, Kruhoffer M, Sorensen FB, Andersen CL, Laiho P, et al. Differential expression of DHHC9 in microsatellite stable and unstable human colorectal cancer subgroups. *British journal of cancer*. 2007; 96(12):1896–903. Epub 2007/05/24. <https://doi.org/10.1038/sj.bjc.6603818> PMID: 17519897; PubMed Central PMCID: PMC2359975.
10. De I, Sadhukhan S. Emerging Roles of DHHC-mediated Protein S-palmitoylation in Physiological and Pathophysiological Context. *Eur J Cell Biol*. 2018. Epub 2018/04/01. <https://doi.org/10.1016/j.ejcb.2018.03.005> PMID: 29602512.
11. Swarthout JT, Lobo S, Farh L, Croke MR, Greentree WK, Deschenes RJ, et al. DHHC9 and GCP16 constitute a human protein fatty acyltransferase with specificity for H- and N-Ras. *The Journal of biological chemistry*. 2005; 280(35):31141–8. Epub 2005/07/08. <https://doi.org/10.1074/jbc.M504113200> PMID: 16000296.
12. Runkle KB, Kharbanda A, Stypulkowski E, Cao XJ, Wang W, Garcia BA, et al. Inhibition of DHHC20-Mediated EGFR Palmitoylation Creates a Dependence on EGFR Signaling. *Mol Cell*. 2016; 62(3):385–96. Epub 2016/05/08. <https://doi.org/10.1016/j.molcel.2016.04.003> PMID: 27153536; PubMed Central PMCID: PMC4860254.
13. Sharma C, Wang HX, Li Q, Knoblich K, Reisenbichler ES, Richardson AL, et al. Protein Acyltransferase DHHC3 Regulates Breast Tumor Growth, Oxidative Stress, and Senescence. *Cancer research*. 2017; 77(24):6880–90. Epub 2017/10/22. <https://doi.org/10.1158/0008-5472.CAN-17-1536> PMID: 29055014; PubMed Central PMCID: PMC5819883.
14. Draper JM, Smith CD. Palmitoyl acyltransferase assays and inhibitors (Review). *Mol Membr Biol*. 2009; 26(1):5–13. Epub 2009/01/20. <https://doi.org/10.1080/09687680802683839> PMID: 19152182; PubMed Central PMCID: PMC2635919.
15. Uhlen M, Bjorling E, Agaton C, Szigartyo CA, Amini B, Andersen E, et al. A human protein atlas for normal and cancer tissues based on antibody proteomics. *Molecular & cellular proteomics: MCP*. 2005; 4(12):1920–32. Epub 2005/08/30. <https://doi.org/10.1074/mcp.M500279-MCP200> PMID: 16127175.

16. Marygold SJ, Leyland PC, Seal RL, Goodman JL, Thurmond J, Strelets VB, et al. FlyBase: improvements to the bibliography. *Nucleic Acids Res.* 2013; 41(Database issue):D751–7. Epub 2012/11/06. gks1024 [pii] <https://doi.org/10.1093/nar/gks1024> PMID: 23125371; PubMed Central PMCID: PMC3531214.
17. Bannan BA, Van Etten J, Kohler JA, Tsoi Y, Hansen NM, Sigmon S, et al. The Drosophila protein palmitoylome: characterizing palmitoyl-thioesterases and DHHC palmitoyl-transferases. *Fly.* 2008; 2(4):198–214. Epub 2008/08/23. PMID: 18719403; PubMed Central PMCID: PMCPMC2898910.
18. He M, Abdi KM, Bennett V. Ankyrin-G palmitoylation and betaII-spectrin binding to phosphoinositide lipids drive lateral membrane assembly. *The Journal of cell biology.* 2014; 206(2):273–88. Epub 2014/07/23. <https://doi.org/10.1083/jcb.201401016> PMID: 25049274; PubMed Central PMCID: PMCPMC4107783.
19. Bruckner K, Perez L, Clausen H, Cohen S. Glycosyltransferase activity of Fringe modulates Notch-Delta interactions. *Nature.* 2000; 406(6794):411–5. Epub 2000/08/10. <https://doi.org/10.1038/35019075> PMID: 10935637.
20. Percher A, Ramakrishnan S, Thinon E, Yuan X, Yount JS, Hang HC. Mass-tag labeling reveals site-specific and endogenous levels of protein S-fatty acylation. *Proceedings of the National Academy of Sciences of the United States of America.* 2016; 113(16):4302–7. Epub 2016/04/05. <https://doi.org/10.1073/pnas.1602244113> PMID: 27044110; PubMed Central PMCID: PMCPMC4843475.
21. Bilder D, Li M, Perrimon N. Cooperative regulation of cell polarity and growth by Drosophila tumor suppressors. *Science.* 2000; 289(5476):113–6. Epub 2000/07/07. PMID: 10884224.
22. Yang CC, Graves HK, Moya IM, Tao C, Hamaratoglu F, Gladden AB, et al. Differential regulation of the Hippo pathway by adherens junctions and apical-basal cell polarity modules. *Proceedings of the National Academy of Sciences of the United States of America.* 2015; 112(6):1785–90. Epub 2015/01/28. <https://doi.org/10.1073/pnas.1420850112> PMID: 25624491; PubMed Central PMCID: PMCPMC4330745.
23. Wurtzel JG, Kumar P, Goldfinger LE. Palmitoylation regulates vesicular trafficking of R-Ras to membrane ruffles and effects on ruffling and cell spreading. *Small GTPases.* 2012; 3(3):139–53. Epub 2012/07/04. <https://doi.org/10.4161/sgtp.21084> PMID: 22751447; PubMed Central PMCID: PMCPMC3442799.
24. Thompson CA, Karelis J, Middleton FA, Gentile K, Coman IL, Radoeva PD, et al. Associations between neurodevelopmental genes, neuroanatomy, and ultra high risk symptoms of psychosis in 22q11.2 deletion syndrome. *Am J Med Genet B Neuropsychiatr Genet.* 2017; 174(3):295–314. Epub 2017/02/01. <https://doi.org/10.1002/ajmg.b.32515> PMID: 28139055.
25. Mukai J, Tamura M, Fenelon K, Rosen AM, Spellman TJ, Kang R, et al. Molecular substrates of altered axonal growth and brain connectivity in a mouse model of schizophrenia. *Neuron.* 2015; 86(3):680–95. Epub 2015/04/29. <https://doi.org/10.1016/j.neuron.2015.04.003> PMID: 25913858; PubMed Central PMCID: PMCPMC4603834.
26. Mukai J, Dhillia A, Drew LJ, Stark KL, Cao L, MacDermott AB, et al. Palmitoylation-dependent neurodevelopmental deficits in a mouse model of 22q11 microdeletion. *Nature neuroscience.* 2008; 11(11):1302–10. Epub 2008/10/07. <https://doi.org/10.1038/nn.2204> PMID: 18836441; PubMed Central PMCID: PMCPMC2756760.
27. Sudo H, Tsuji AB, Sugyo A, Ogawa Y, Sagara M, Saga T. ZDHC8 knockdown enhances radiosensitivity and suppresses tumor growth in a mesothelioma mouse model. *Cancer Sci.* 2012; 103(2):203–9. Epub 2011/10/25. <https://doi.org/10.1111/j.1349-7006.2011.02126.x> PMID: 22017350.
28. Gao X, Pan D. TSC1 and TSC2 tumor suppressors antagonize insulin signaling in cell growth. *Genes Dev.* 2001; 15(11):1383–92. <https://doi.org/10.1101/gad.901101> PMID: 11390358.
29. Chen B, Zheng B, DeRan M, Jarugumilli GK, Fu J, Brooks YS, et al. ZDHC7-mediated S-palmitoylation of Scribble regulates cell polarity. *Nature chemical biology.* 2016; 12(9):686–93. Epub 2016/07/06. <https://doi.org/10.1038/nchembio.2119> PMID: 27380321; PubMed Central PMCID: PMCPMC4990496.
30. Murphy J, Kolandaivelu S. Palmitoylation of Progressive Rod-Cone Degeneration (PRCD) Regulates Protein Stability and Localization. *The Journal of biological chemistry.* 2016; 291(44):23036–46. Epub 2016/10/30. <https://doi.org/10.1074/jbc.M116.742767> PMID: 27613864; PubMed Central PMCID: PMCPMC5087724.
31. Sharma C, Rabinovitz I, Hemler ME. Palmitoylation by DHHC3 is critical for the function, expression, and stability of integrin alpha6beta4. *Cell Mol Life Sci.* 2012; 69(13):2233–44. Epub 2012/02/09. <https://doi.org/10.1007/s00018-012-0924-6> PMID: 22314500; PubMed Central PMCID: PMCPMC3406256.
32. Brand AH, Perrimon N. Targeted gene expression as a means of altering cell fates and generating dominant phenotypes. *Development.* 1993; 118(2):401–15. PMID: 8223268.

33. Venken KJ, Schulze KL, Haelterman NA, Pan H, He Y, Evans-Holm M, et al. MiMIC: a highly versatile transposon insertion resource for engineering *Drosophila melanogaster* genes. *Nature methods*. 2011; 8(9):737–43. Epub 2011/10/11. PMID: [21985007](#); PubMed Central PMCID: PMC3191940.
34. Baena-Lopez LA, Alexandre C, Mitchell A, Pasakarnis L, Vincent JP. Accelerated homologous recombination and subsequent genome modification in *Drosophila*. *Development*. 2013; 140(23):4818–25. Epub 2013/10/25. <https://doi.org/10.1242/dev.100933> PMID: [24154526](#); PubMed Central PMCID: PMC3833436.
35. Tiebe M, Lutz M, De La Garza A, Buechling T, Boutros M, Teleman AA. REPTOR and REPTOR-BP Regulate Organismal Metabolism and Transcription Downstream of TORC1. *Developmental cell*. 2015; 33(3):272–84. <https://doi.org/10.1016/j.devcel.2015.03.013> PMID: [25920570](#); PubMed Central PMCID: PMC4430829.
36. Wan J, Roth AF, Bailey AO, Davis NG. Palmitoylated proteins: purification and identification. *Nature protocols*. 2007; 2(7):1573–84. Epub 2007/06/23. <https://doi.org/10.1038/nprot.2007.225> PMID: [17585299](#).
37. Gramates LS, Marygold SJ, Santos GD, Urbano JM, Antonazzo G, Matthews BB, et al. FlyBase at 25: looking to the future. *Nucleic Acids Res*. 2017; 45(D1):D663–D71. Epub 2016/11/02. <https://doi.org/10.1093/nar/gkw1016> PMID: [27799470](#); PubMed Central PMCID: PMC5210523.